ISSN 1682-296X (Print)
ISSN 1682-2978 (Online)

Bio Technology

ANSInet
Asian Network for Scientific Information
308 Lasani Town, Sargodha Road, Faisalabad - Pakistan

Biotechnology 5 (1): 42-48, 2006
ISSN 1682-296X

A Device for the Targeting Delivery of Particulate DNA Vaccines

Yi Liu
The PowderJect Centre for Gene and Drug Delivery Research,
Department of Engineering Science, University of Oxford,
Oxford OX1 3PJ, United Kingdom

Abstract: A unique biomedical device, the hand-held powdered injection system (biolistics), is proposed for the targeting delivery of DNA vaccines. The underlying principle is to harness energy of high-pressure helium to accelerate a pre-measured dose of DNA vaccine coated in microgold particles to an appropriate momentum in order to penetrate the outer layer of the skin or mucosal tissue to achieve a biological effect. The novelty of this hand-held biolistics, using the venturi effect to entrain micron-sized vaccines into an established quasi-steady Supersonic Jet Flow (QSSJF) and accelerate them towards the target. In this paper, Computational Fluid Dynamics (CFD) is utilized to characterize of prototype biolistic system. The key features of the gas dynamics and gas-particle interaction are presented. The overall capability of the biolistic system to deliver the particles is discussed. The statistic analyses show the particle impact velocity is achieved 745 m s^{-1} for representative gold particles.

Key words: Biolistics, device, DNA vaccination, impact, particle, supersonic nozzle

INTRODUCTION

DNA vaccination offers a promising new therapeutic intervention for a wide range of diseases. Gene gun immunization propels DNA-coated particles into the human skin, is proven to achieve efficient transfection of a number of cell types, with intracellular DNA delivery (Chen *et al*., 2002; Trimble *et al*., 2003; Vessilev *et al*., 2001).

The skin is the largest organ in the body, comprising about 16% of the body's weight, has a average surface area of ~1.8 m^2. It serves many important functions, including regulating body temperature, maintaining water and electrolyte balance and sensing painful and pleasant stimuli. The skin keeps dangerous substances from entering the body and provides a shield from the sun's harmful effects. More importantly, the skin performs a complex role in human immunity system.

Figure 1 schematically shows the skin structure, consisting of three functional layers, namely, epidermis, dermis and subcutis (hypodermis). The keratinised epidermal cells with their tight conjunction form the stratum corneum. This physical structure prevents molecules more than nominal filter rating of 500 Da to penetrate. The underlying viable epidermis, with its dense network of antigen-presenting cells (Langerhans cells, shown in Fig. 2) and relative lack of sensory nerve endings, has long been recognized as a safe and effective target tissue for vaccination (Chen *et al*., 2002). The most common administration for human vaccines injection is the intramuscular vaccine injection, despite of its inefficient immune responses. In contrast, skin, a potent immunological induction site, is rarely used for vaccination because of its poor accessibility by needle and its poor permeability to topically applied vaccines.

To this end, we are developing a controllable hand-held powdered injection system (biolistic), which harnesses energy of compressed helium gas to accelerate the micro-sized vaccines to sufficient momentum to penetrate the outer layer of skin or mucosal tissue to target the cells of interest (Bellhouse *et al*., 1994; Liu *et al*., 2002; Costing *et al*., 2004). It can deliver particles locally with a velocity range and spatial distribution preferable for DNA vaccine administration. Both humoral (antibodybased defenses in blood and lymph systems) and cell-mediated immunities (CTL responses) are demonstrated in animals using this technology (Chen *et al*., 2002). Figure 3 shows a typical skin photo following the biolistic delivery.

In this study we explore the performance of one of experimental biolistic delivery systems. The objective is to characterize the prototype biolistic device with both experiment techniques and numerical approaches, with the primary emphasis on the interaction between the gas and the particles.

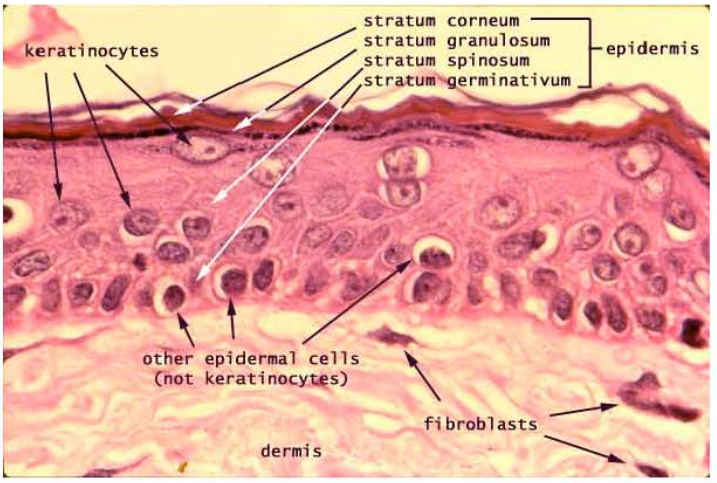

Fig. 1: Schematic drawing (transverse section) of human skin, illustrating the epidermis, dermis, subcutis and major cellular components. http://www.siumed.edu/~ dking2/intro/skin.htm)

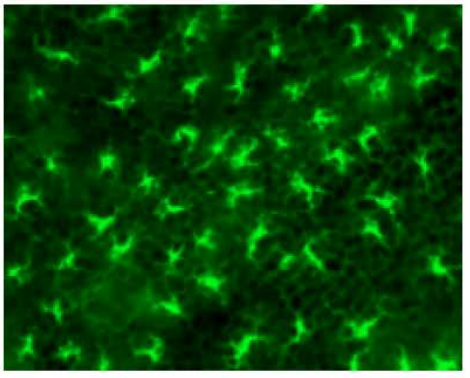

Fig. 2: Plane view of Langerhans cells, star-shaped resident immune cells

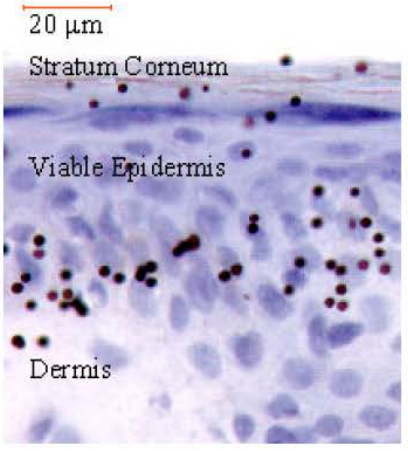

Fig. 3: A typical skin photo following the particle delivery

MATERIALS AND METHODS

The biolistic device: Figure 4 shows a variant of clinical hand-held bilolistic device, utilizing a quasi-steady quasi-one dimensional transonic flow behind a propagating shock wave to accelerate particles and to impact the skin target.

Upon actuation, high-pressure helium is released from the gas-cylinder, a large pressure difference builds up across the diaphragm, which leads to the formation of a shock wave. This primary shock wave propagates downstream to the supersonic nozzle, initiating an unsteady gas flow, as in a classical shock tube. Subsequently, a sustained quasi-steady supersonic flow regime is established. In the course of these processes, particles are entrained and accelerated towards the nozzle exit. As the gas-particle flow impinges on the skin target, gas is deflected away and vented to the atmosphere through a silencer. The particles, with their relatively large inertia, maintain a high velocity and penetrate the stratum corneum and target the cells of interest.

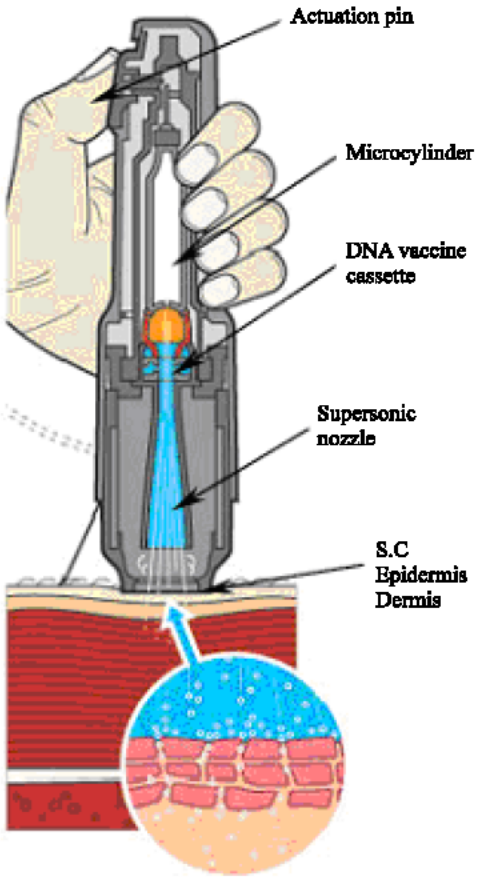

Fig. 4: A hand-held shock-tube based biolistic device

In this study, we proposed a experimental biolistic system (biolistic), which has been used in various studies both *in vitro* and *in vivo* with satisfactory results (Bellhouse *et al*., 1994; Liu *et al*., 2002; Costing *et al*., 2004). The key feature is the use of venturi effects to entrain powdered vaccines into an established quasi-steady high speed gas jet flow, so that no diaphragm is required to retain the particles and potentially avoids the fragment carryovers. All vaccine particles are accelerated by a continuous high speed jet flow in the biolistic device over a period of <3 ms, targeting specific skin or mucosal cells.

Characterization of the biolistic device

Configuration and experimental setup: The prototype biolistic device under experimental investigations is illustrated schematically in Fig. 5. The 4 MPa gas-cylinder is used. The cassette is loaded with a powdered payload of 1.0 mg. The model particles for numerical simulation and experimental studies were gold spheres with a density of 19,920 kg m^{-3} and the diameter of 1.8 μm, which are representative of intercellular DNA vaccine delivery applications.

Since the emphasis is on the events after the supersonic jet being established and on the area from downstream of the sonic throat, the course of gas released from the cylinder is not simulated. Instead, the measured pressure history at the position P* is taken in as the inlet total pressure.

Numerical method: A commercial CFD software, Fluent (Http://www.fluent.com/), is chosen to numerically simulate the gas and particles flow of the prototype biolistic system. A coupled explicit solver is selected in order to capture the main features of the unsteady motion of the shock wave process. An overall second order accuracy is satisfied both spatially and temporally to accurately predict the interaction between the oblique shock and the turbulence boundary layer. Given the nature of the biolistic system and the required accuracy, the standard k-ε turbulence model, is used. It has been proven robust, economical and accurate for a wide range of turbulent flows in many industrial applications and the shock-tube based devices. A non-equilibrium wall function is employed to consider the effects of pressure gradient and strong non-equilibrium in the near-wall region of the biolistic device.

The transient gas flow and its interaction with particles are modelled simultaneously and interactively. The solution of multi-species gas phase is obtained by numerically solving the 2D axisymmetric Reynolds-averaged Navier-Stokes (RANS) equations, together with

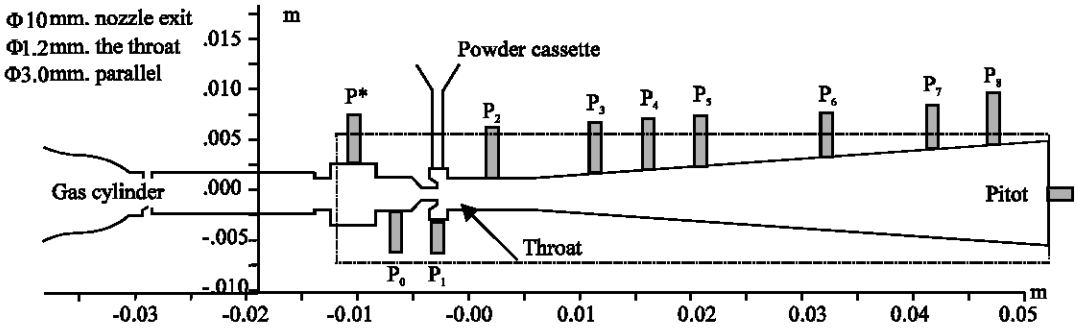

Fig. 5: Configuration of the prototype biolistic device and the experimental setup

turbulence model and species transport equation. The particle velocity is obtained over discrete time steps along the trajectory. The trajectories, in conjunction with the drag correlation of Igra and Takayama, are advanced in time with gas flow simulation. The inter-phase exchange of momentum and heat is also considered in each time step. Further details can be found in the literature (Liu *et al*., 2002; Liu and Kendall, 2004a, 2004b; Liu and Costigan, 2005; Liu and Kendall, 2004c).

The computational domain is extended to 80D×40D (where D is diameter of the sonic throat) to accommodate the non-reflected boundary condition imposed, with total of 22444 cells. The mesh is concentrated near the wall and well placed in the region of interest. The simulation is initialized with the air at atmospheric pressure and room temperature. The mixture gas of high-pressure helium initially stored in the gas-cylinder with the residual air at atmospheric pressure is imposed as the inlet flow. Atmospheric pressure is specified at the outlet boundary for the subsonic outflow. The device wall temperature is assumed constant during the particle delivery (usually < 3 ms of interest), with a non-slip velocity condition imposed. The non-reflected condition is set for the far field boundaries.

This study was conducted in the PowderJect Centre for Gene and Drug Delivery Research, University of Oxford, in collaboration with Chiron vaccines.

RESULTS

Simulations with different combination of grids, physical models and particle drag correlations are carried out to ensure grid-independent solutions and to evaluate the drag correlations for the micro particle in the transient supersonic jet flow.

Figure 6 shows the calculated and experimental time histories of the static pressure, with the locations marked in Fig. 5. The pressure measurements here are averaged value over an area of 1.8 mm in diameter (the size of the pressure transducer).

The calculated static pressures in Positions P_4 and P_8 before the time of 200 μs are higher than those measured and are also quite oscillatory. This is probably due to the mismatch of the inlet boundary conditions, since no measurement of the inlet total pressure or temperature is available. Rather, the pressure trace from the pressure transducer in Position P* was taken as the total pressure. However, as indicated in Fig. 6a, this discrepancy, due to the boundary condition treatment, is unnoticeable from 250 μs when the supersonic jet flow is established.

In general, it shows good agreement between numerical simulations and experimental measurements.

Figure 7 reveals the two-dimensional flow field, in the form of velocity contours at the time of 1.1 ms. In Fig. 7a, we can clearly see the supersonic core flow region, with a high velocity in the central area and a quite low velocity towards the nozzle wall. The oblique shock repeatedly interacts with and is reflected from the wall in the parallel section and the diverging nozzle. The interactions become progressively weaker as it propagates to the nozzle exit. This is consistent with the velocity distributions (Fig. 8). The equivalent PIV measured velocity map are shown in Fig. 7b. They are coincident in terms of the velocity range and its contours.

The calculated velocity profiles at 1 mm downstream of the nozzle exit plane are presented in Fig. 8 at the time of 1 ms. The measured mean velocity and the standard deviation are plotted for a comparison. It can be observed that the coring feature becomes evident, with no more than 5 mm in diameter for the gas velocity above 500 m s^{-1}, which is considered to have a sufficient momentum to accelerate the particles (as it will be demonstrated by the particle simulation results). This is largely due to the over-expanded nozzle operation condition.

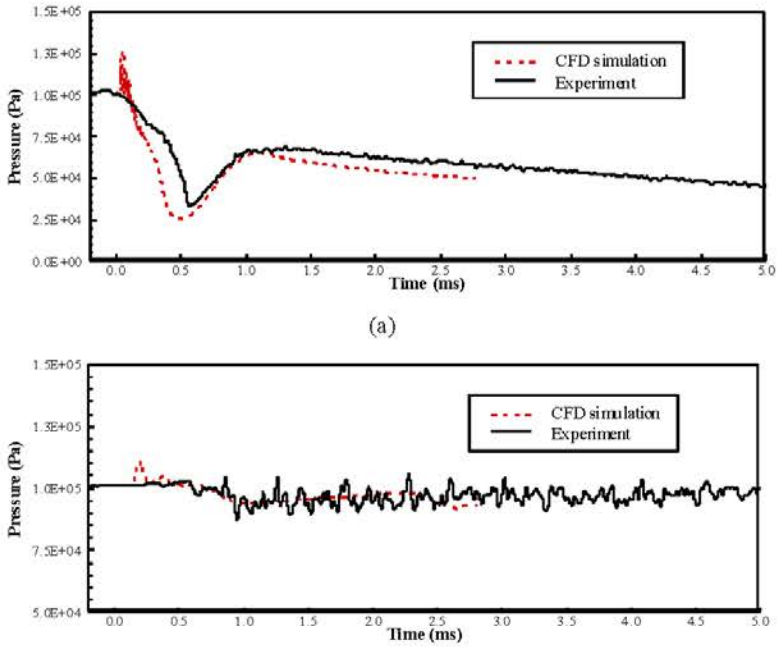

(a)

(b)

Fig. 6: Comparison of simulated and experimental pressure histories at P_4 (a) and P_8 (b) Positions of)

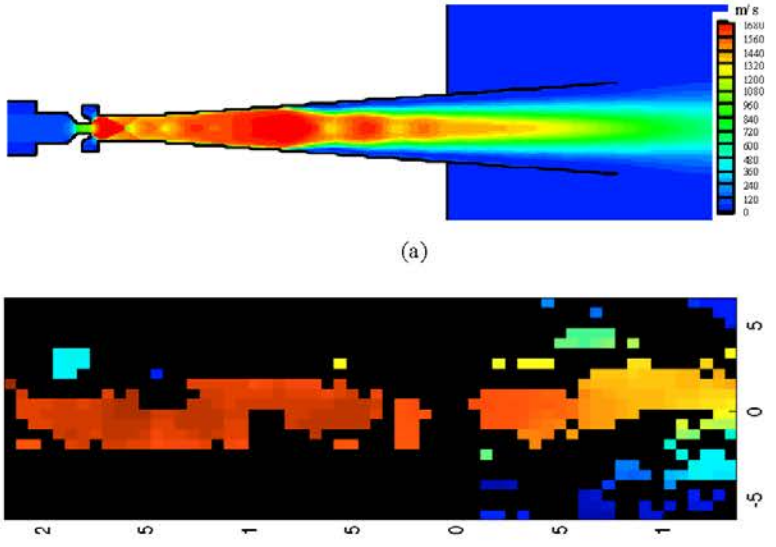

(a)

(b)

Fig. 7: (a) Computed velocity contours (b) PIV measured velocity map of the flow field at the time of 1.1 m s^{-1}

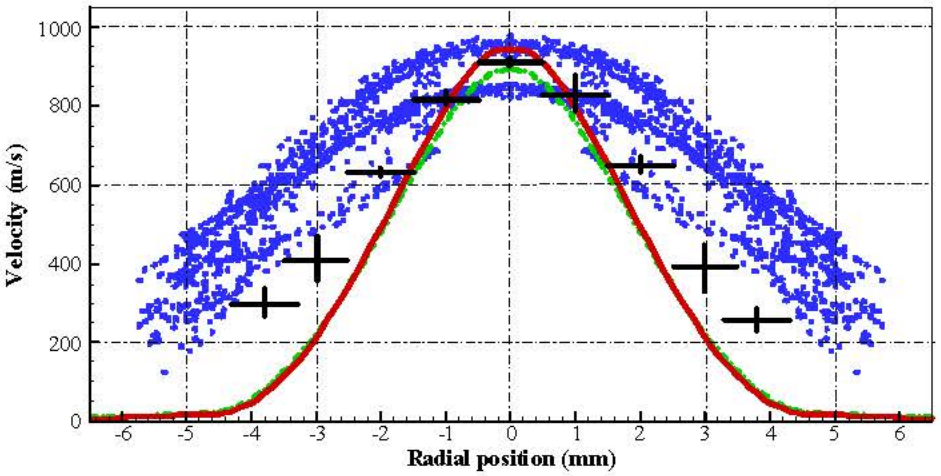

Fig. 8: The velocity profiles at 1 mm downstream of the nozzle exit plane (solid line: computed gass velocity, dot:particle velocity, measurements marked too)

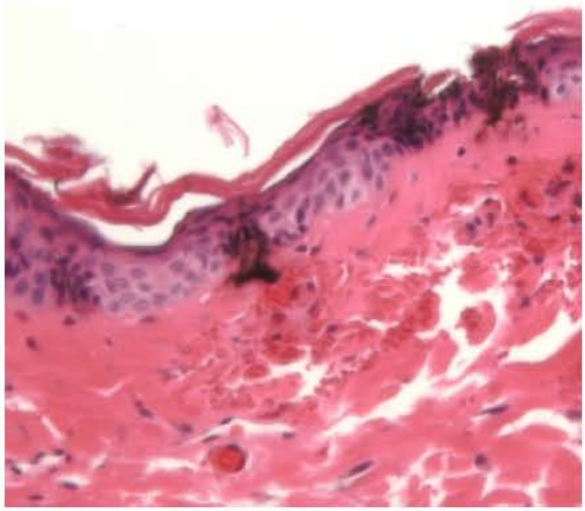

Fig. 9: A histological photomicrograph of gold particle delivery into the mouse

Not surprisingly, a higher particle velocity is seen to be restricted in the central core region of the diameter of ~ 5 mm, similar to the gas flow field (Fig. 7a, too), when we extract the calculated particle velocity data and plot them in Fig. 8. The particle velocity in the free jet exhibits a wide range, 400-1,000 m s^{-1} and with few particles distributed in the outside area. This is consistent with the gas velocity distribution. The mean velocity of 745.0 m s^{-1}, with the stand deviation of 172.50 m s^{-1}, is obtained for particle velocity analyses.

The DNA-coated gold particles are directly delivered into the Langerhans cell following the biolistic immunization. Figure 9 shows a histological photomicrograph of gold particles delivered to mouse skin.

DISCUSSION

A new device has proposed and characterized for targeting delivery micro-size DNA vaccines into the human skin. Transient gas and particles dynamics within a prototype biolistic system have been investigated experimentally and numerically.

Simulated pressure histories and velocity distributions agree well with the corresponding pressure transducer and PIV measurements. The gas and particles interactions have been calculated by implementing the drag correlation within the modeled gas flow field. The analyses show the particle velocity is achieved about 400-1000 m s^{-1} for representative gold particles (1.8 μm in diameter), with the mean velocity, 745.0 m s^{-1}. It is

demonstrated the prototype device can deliver particles with a favourable velocity range and spatial distribution for DNA vaccine administration.

ACKNOWLEDGMENTS

The author wish to thank Professor Brian J. Bellhouse for his enthusiastic contributions and support and Chiron Vaccines for funding this work. Dr. George Costigan and Dr. Fiona Carter are acknowledged for the permission of using their experimental data.

REFERENCES

Bellhouse, B.J., D.F. Sarphie and J.C. Greenford, 1994. Needless syringe using supersonic gas flow for particle delivery. Intl. Patent WO94/24263.

Chen, D., Y. Maa and J.R. Haynes, 2002. Needle-free epidermal powder. Expert Review of Vaccines, 1: 89-100.

Costigan, G., Y. Liu, G.L. Brown, F.V. Carter and B.J. Bellhouse, 2004. Evolution of the design of the biolistic devices for the delivery of dry particles to skin or mucosal tissue. Proceeding of 24th Intrenational Symposium on Shock Waves, Paper-2981, Beijing, PR China

Fluent user's guide volume, Fluent inc., Lebanon, NH 03766, USA. Also see Http://www.fluent.com/

Liu, Y., M.A.F. Kendall, N.K. Truong and B.J. Bellhouse, 2002. Numerical and experimental analysis of a high speed needle-free powdered vaccines delivery device, AIAA-2002-2807. Proceeding of 20th AIAA Applied Aerodynamics Conference, St. Louis, USA

Liu, Y. and M.A.F. Kendall, 2004a. Numerical simulation of heat transfer from a transonic jet impinging on skin for needle-free powdered drug and vaccine delivery. Journal of Mechanical Engineering Science, Proceedings of the Institution of Mechanical Engineers Part C. 218: 1373-1383.

Liu, Y. and M.A.F. Kendall, 2004b. Numerical study of a transient gas and particle flow in a high-speed needle-free ballistic particulate vaccine delivery system. Journal of Mechanics in Medicine and Biology, 4: 559-578.

Liu, Y. and M.A.F. Kendall, 2004c. Needle-free drug injections, Fluent Newsletters. Http://www.fluent.com/about/news/newsletters/04v13i1/s7.htm

Liu, Y. and G. Costigan, 2005. Aerodynamic performance of an earlier venturi powdered vaccines/drug delivery system, AIAA-2005-5005, Proceeding of 35th AIAA Fluid Dynamics Conference and Exhibit, Toronto, Canada

Trimble, C., C. Lin, C. Hung, S. Pai, J. Juang and L. He, 2003. Comparison of the CD8+ T cell responses and antitumor effects generated by DNA vaccine administered through gene gun, biojector and syringe. Vaccine, 21: 4036-4042.

Vassilev, V.B., L.H.V.G. Gil and R.O. Donis, 2001. Microparticle-mediated RNA immunization against bovine viral diarrhea virus. Vaccine, 19: 2012-2019.